



Theoretical and experimental investigations of structural and electronic properties of some quinoxalin-2(1H)-one derivatives

R. Jdaa¹, A. El Assry^{1*}, B. Benali¹

¹Laboratory of Optoelectronic, Physical Chemistry of Materials and Environment, Department of Physics, Faculty of Science, Ibn Tofail University, PB.133, Kenitra, Morocco

Received 22Feb2018,
Revised 23Feb 2018,
Accepted 25 Mar 2018

Keywords

- ✓ Quinoxalin-2(1H)-one,
- ✓ DFT/3BLYP/6-31G(d, p),
- ✓ Geometric parameters,
- ✓ Atomic charges,
- ✓ Electronic density,
- ✓ Electrostatic potentials,
- ✓ Dipolar moments.

abdeslam_elassry@yahoo.fr

Phone: +212662662468;

Abstract

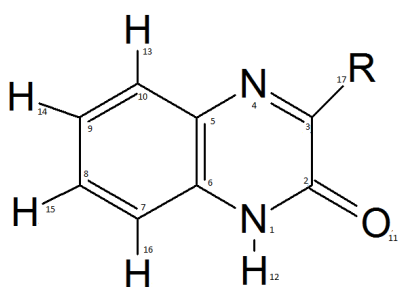
The quantum computations using the DFT/3BLYP/6-31G(d, p) level method are performed to optimize geometries and obtain some molecular properties for quinoxalin-2(1H)-one, 3-methylquinoxalin-2(1H)-one and 3-benzylquinoxalin-2(1H)-one. The results indicate a strong polarization between the heterocyclic and aromatic rings, which largely determines the expected reactivity. Atomic charges, electronic density, electrostatic potentials, HOMO and LUMO energy and dipole moments allowed the extension of qualitative predictions about the reactivity of these derivatives.

1. Introduction

Quinoxalin-2(1H)-one is a molecule consisting of two rings: one is aromatic; the other contains two intracyclic heteroatoms and one ketone (compound Q₁ of Figure 1). In recent years, researchers have been interested in studying the properties of this molecule and its derivatives because of their uses in the pharmacological field. We have been interested in the molecular properties of these compounds because several publications have recently reported that some quinoxalin-2(1H)-one are the highly effective NMDA receptor antagonists [1- 3]. Thus, achieving the water solubility of quinoxalin-2(1H)-one without loss of selectivity and potency profiles becomes an important challenge for medicinal chemistry [4]. This challenge motivated research on methods of substituted quinoxalin-2(1H)-one [5- 11]. recently, studied intensively, and the study of structural and energetic properties of Quinoxalines derivatives has been done by our group[12-16]. Because of this pharmacological interest, and in the absence of fundamental spectroscopic data in the literature on these compounds, we have found it useful to discuss some of their molecular properties of potential interest. The latter could further explore the reactivity and mechanisms involving the part of quinoxalin-2(1H)-one in biological systems such as those mentioned above, The detailed crystal data on 2-OHQ has been reported previously by Padjama et al. [17], and 3-methylquinoxalin-2(1H)-one has been reported previously by Mondieig et al. [18]. For this purpose, we have studied the molecular properties of the three compounds of Fig. 1, ie the quinoxalin-2(1H)-one itself as well as its two derivatives: 3-methylquinoxalin-2(1H)-one and 3-benzylquinoxalin-2(1H)-one.

2. Theoretical Methodology

DFT methods were used in this study. These methods have become very popular in recent years [19,20]because they can achieve a precision similar to other methods (AM1, CNDO, HF: quantitative relations structure-activity) in less time and less expensive from a computer point of view.



Compound	R
Q ₁	H
Q ₂	CH ₃
Q ₃	PhCH ₂

Figure 1 : General formula for quinoxalin-2(1H)-one derivatives studied in this work

In agreement with the DFT results, the ground state energy of a polyelectronic system can be expressed by the total electron density, and in fact, the use of electron density instead of wave function to compute the energy constitutes the fundamental basis of the DFT [21]. Molecular geometries were optimized using analytical gradients in DFT calculations with Gaussian RHF hybrid functional bases. This level of theory is known to provide reliable theoretical results for medium-sized organic compounds in quantum calculations that include electronic correlation at a moderate computational effort [22]. Optimization of geometry was performed for compound 1 with symmetry restrictions to maintain the regular hexagonal structure in the phenyl ring. Then, we complete the work with a discussion of the effect of methyl or benzyl substitution (R17) on the behavior of the structural and energetic properties of the base molecule. Insofar as the structures thus obtained provide sufficiently reliable models of the molecules under consideration, the properties studied should not change substantially when fully optimized geometries should be used instead. The electron density DFT was obtained in punctual calculations at these geometries for the subsequent atoms in the molecules (AIM) [23, 24] and the natural orbital analyzes (NBO) [25] as well as for the determination of the electrostatic potentials [26].

The AIM theory developed by Bader and his colleagues [23] since the early 1970s has become a mature theory firmly rooted in quantum mechanics and currently widely used as a rigorous and elegant tool for extracting much information of interest into chemistry. The theory has been extensively expounded by Bader and reviewed at the introductory level by Popelier [24], so we briefly present the particular properties considered here. The NBO analysis put forward by Weinhold et al. [25, 28] uses the single-electron density matrix to define the atomic orbital in the molecular environment and to derive $\rho(r)$ bonds between the atoms. It applies an orthogonalization scheme to define an orthonormal basis in which the matrix representation of the mono-electronic matrix is diagonal [28]. The orbitals of this orthonormal ensemble are the natural orbitals and the diagonal elements of the density matrix in this base are the orbital populations [25, 28]. The sum of all orbital contributions belonging to a given center gives its atomic charge of natural population analysis (NPA). From abundant literature on different population patterns for the atomic computation of charges in organic molecules, a consensus has been reached in recent years on the superiority of NPA and AIM charges not only for their firm theoretical reasons, but also for their stability and their good performance on conformational and structural changes [31, 32]. All the calculations were performed with the Gaussian 09 packages [33]. The density functional theory (DFT) with Becke's three parameter functional and the Lee–Yang–Parr functional (B3LYP) [32–34] and 6-31G(d,p) basis set was employed to investigate the structure optimization of the ground state of the dyes in gas phase.

3. Results and discussion

3-1. Experimental

The products used, Q₁, Q₂ and Q₃ (Fig. 1), are synthesized by the methods described in reference [35], we have found at room temperature that the Q₁ have a single-crystal structure of quinoxalin-2(1H)-one (C₈H₆N₂O). The compound is Orthorhombic P212121, with Z = 4. The unit-cell dimensions are a = 21.318 (3) Å, b = 7.350 (1) Å and c = 4.350 (1) Å, the density is d = 1.424 g.cm⁻³ and the volume equal to 681.6 Å³. For the Q₂ compound a single-crystal structure of 3-méthylquinoxalin-2(1H)-one (C₉H₈N₂O) was determined at room temperature. The compound is monoclinic, with space group is P21/c and Z = 4. The unit-cell dimensions are a = 4.050 (2) Å, b = 11.240(2) Å, c = 16.975(5) Å, and $\beta = 91.38(3)^\circ$ the density is d = 1.377 g.cm⁻³ and V = 772.5 Å³. For Q₃ the single-crystal structure of 3-benzylquinoxalin-2(1H)-one (C₁₅H₁₂N₂O) was determined. The compound is monoclinic, P2₁/c with Z = 4. The unit-cell dimensions are a = 12.752(2) Å, b = 4.820(1) Å, c = 19.699(3) Å, and $\beta = 93.54(1)^\circ$ the density is 1.298g.cm⁻³ and the volume equal to 1208.5 Å³.

3-2. Geometrical parameters

Table 1 reveals the bond length (Å) of the studied quinoxalinone derivatives **Q₁**, **Q₂** and **Q₃** calculated at Methods (AM1, CNDO, HF and DFT/B3LYP) using four basis sets 6-31G(d,p) in gas phase.

Table 1: Bond length (Å) of the studied quinoxalinone derivatives **Q₁**, **Q₂** and **Q₃** calculated at Methods (AM1, CNDO, HF and DFT/B3LYP) using four basis sets 6-31G(d,p) in gas phase.

Methods	AM1	CNDO	HF	(DFT) B3LYP	AM1	CNDO	HF	(DFT) B3LYP	(DFT) B3LYP	X-Ray [6]	X-Ray [7]
Bond lengths (Å)	Q₁	Q₁	Q₁	Q₁	Q₂	Q₂	Q₂	Q₂	Q₃	Q₁	Q₂
r(N ₁ C ₂)	1.397	1.381	1.361	1.388	1.395	1.379	1.358	1.383	1.383	1.342	1.345
r(N ₁ C ₆)	1.393	1.391	1.383	1.383	1.392	1.391	1.383	1.384	1.383	1.372	1.380
r(C ₂ C ₃)	1.494	1.435	1.487	1.481	1.505	1.446	1.499	1.493	1.492	1.465	1.482
r(C ₂ O ₁₁)	1.242	1.280	1.197	1.223	1.243	1.281	1.199	1.225	1.227	1.239	1.239
r(C ₃ N ₄)	1.294	1.305	1.261	1.291	1.303	1.316	1.265	1.296	1.295	1.287	1.291
r(C ₃ R ₁₇)	1.105	1.118	1.076	1.088	1.492	1.455	1.498	1.498	1.510	1.485
r(N ₄ C ₅)	1.405	1.394	1.392	1.389	1.402	1.392	1.391	1.388	1.387	1.386	1.387
r(C ₅ C ₆)	1.435	1.408	1.393	1.416	1.433	1.408	1.391	1.414	1.414	1.411	1.400
r(C ₅ C ₁₀)	1.413	1.399	1.392	1.405	1.414	1.399	1.392	1.405	1.405	1.402	1.398
r(C ₆ C ₇)	1.415	1.397	1.391	1.402	1.415	1.396	1.391	1.401	1.401	1.401	1.393
r(C ₇ C ₈)	1.383	1.378	1.377	1.388	1.383	1.379	1.378	1.389	1.389	1.363	1.368
r(C ₈ C ₉)	1.401	1.390	1.393	1.404	1.401	1.390	1.393	1.403	1.404	1.403	1.401
r(C ₉ C ₁₀)	1.384	1.378	1.376	1.386	1.383	1.378	1.377	1.387	1.387	1.373	1.365

The Bond angle in (°) calculated at DFT/B3LYP using four basis sets 6-31G(d,p) in gas phase are presented in table 2.

Table 2: Bond angle in (°) of the studied quinoxalinone derivatives **Q₁**, **Q₂** and **Q₃** calculated at DFT/B3LYP using four basis sets 6-31G(d,p) in gas phase.

Valance Angles (°)	Q₁	Q₂	Q₃	Q₁ X-Ray [6]
θ(C ₂ N ₁ C ₆)	124.202	124.383	124.499	122.5
θ(C ₂ N ₁ H ₁₂)	115.652	115.409	115.323	-----
θ(N ₁ C ₂ C ₃)	112.835	113.750	113.624	115.6
θ(N ₁ C ₂ O ₁₁)	122.518	122.116	121.795	121.8
θ(C ₃ C ₂ O ₁₁)	124.645	124.133	124.575	122.6
θ(C ₂ C ₃ N ₄)	125.464	123.522	123.514	124.8
θ(C ₂ C ₃ R ₁₇)	115.401	115.986	116.609	-----
θ(N ₄ C ₃ R ₁₇)	119.134	120.491	119.870	-----
θ(C ₃ N ₄ C ₅)	118.603	119.649	119.810	117.5
θ(N ₄ C ₅ C ₆)	121.555	121.795	121.627	121.4
θ(N ₄ C ₅ C ₁₀)	119.339	119.347	119.488	119.2
θ(C ₆ C ₅ C ₁₀)	119.105	118.856	118.884	119.4
θ(N ₁ C ₆ C ₅)	117.338	116.899	116.917	118.3
θ(N ₁ C ₆ C ₇)	122.395	122.548	122.516	122.3
θ(C ₅ C ₆ C ₇)	120.266	120.551	120.566	119.4
θ(C ₆ C ₇ C ₈)	119.403	119.355	119.318	119.8
θ(C ₇ C ₈ C ₉)	120.922	120.773	120.793	120.8
θ(C ₈ C ₉ C ₁₀)	119.766	119.859	119.876	120.0
θ(C ₅ C ₁₀ C ₉)	120.536	120.603	120.560	120.6

Table 3 exhibit the Bond torsion in (°) calculated at DFT/ B3LYP using four basis sets 6-31G(d,p) in gas phase.

Table 3: Bond torsion in ($^{\circ}$) of the studied quinoxalinone derivatives Q_1 , Q_2 and Q_3 calculated at DFT/ B3LYP using four basis sets 6-31G(d,p) in gas phase.

Torsion	Q_1	Q_2	Q_3
$\tau (R_{17}C_3C_4C_5)$	-180.018	-180.015	-178.250
$\tau (C_{10}C_5C_6N_1)$	180.004	180.000	179.692

The phenyl ring has the geometry of a regular hexagonal. the lengths of the bonds are grouped into three categories: (i) $C_7C_8 = C_9C_{10}$, (ii) $C_5C_{10} = C_6C_7 = C_8C_9$ (iii) C_5C_6 of length 1.38, 1.40 and 1.41 Å, while in the cycle which contains the two atoms of nitrogen, only the valence angles $N_4C_5C_6$ and $C_3N_4C_5$ have a value close to that of a regular hexagonal (120°) with an angle $C_6N_1C_2$ increased by 4.20° and the angles $N_1C_2C_3$ decreased by 7.17° because of the inductive effect of the grouping ketone $C=O$ and the angle $N_1C_6C_5$ decreased by 2.67° due to the electronegativity of the two nitrogen atoms N_1 and N_4 .

The substitution of the hydrogen atom in the compound 1 by the methyl group in the molecule 2 and by the benzyl in the molecule 3 causes the length of the C_3-R_{17} bond to increase by 0.42 Å. However the $C_2C_3N_4$ angle undergoes a decrease of about 2° for the compounds 2 and 3. The substitution also leads to the increase of the angles $C_2C_3R_{17}$ and $N_4C_3R_{17}$.

The values of the dihedral angle $C_{10}C_5C_6N_1$ in the three molecules studied are of the order of 180° , which shows that the existence of substituent in position 3 does not affect the flatness of the three molecules. Also, the values of the dihedral angle $R_{17}C_3N_4C_5$ ($\sim 180^{\circ}$) showing that the heteroatoms contribute to electronic delocalization in these molecules.

3-3. Electronic density

In Table 4, we group the local electronic density of the critical points of the BCP bonds (the bonds with the hydrogen atoms in the phenyl ring have been neglected). The values of $\rho_c = \rho(r_c)$ can be used to control growth or decay relative to charge accumulation due to the presence of a substituent when $V_c = V(r_c)$ and includes the effect of the nucleus thereby giving an evaluation of the final electrostatic balance. The general characteristics of the different values in Table 2 are similar to covalent bonds [23, 36]. The values of ρ_c obtained are between 0.2 and 0.6 ua. In order to discuss the particular and distinctive features that flow from Table 2, let's first analyze the effect of substitution on the local value of the electronic density at BCPs: The values of the electronic density of the C bond with the R_{17} group in the 3-methylquinoxalin-2(1H)-one and 3-benzylquinoxalin-2(1H)-one molecules are qualitatively lower than that in quinoxalin-2 (1H)-one of about 5% and 10% respectively.

The low values of the electron density are observed for the bonds N_1C_2 and C_2C_3 in the molecule 1. A slight increase of the value of the electronic density of the bond N_1C_2 and a slight decrease of the value of the electronic density of the bond C_2C_3 were observed for molecules 2 and 3.

Table 4: Local Values of the Electronic Density ρ_c to BCPs for the Compounds in Figure 1 (Compounds 1,2 and 3)

Bond	Q_1	Q_2	Q_3
N_1C_2	0.209915	0.213659	0.223641
C_2C_3	0.335883	0.282033	0.288975
C_2O_{11}	0.573926	0.599138	0.557603
C_3N_4	0.446768	0.484166	0.457003
C_3R_{17}	0.374058	0.354295	0.335582
N_4C_5	0.327618	0.321775	0.325078
C_5C_6	0.444258	0.442443	0.442784
C_6C_7	0.459950	0.459993	0.458236
C_7C_8	0.529120	0.528004	0.527853
C_8C_9	0.523430	0.524169	0.523621
C_9C_{10}	0.527425	0.524531	0.524373
$C_{10}C_5$	0.520705	0.510528	0.509425

Regarding the phenyl ring, it is worth mentioning that the local properties of BCP can be an extremely sensitive way to analyze bonds. The fused ring in quinoxalin-2(1H)-one requires CC bonds in phenyl to be grouped into four categories: i) C_5C_6 , ii) C_6C_7 , iii) C_5C_{10} , (iv) $C_7C_8 = C_8C_9 = C_9C_{10}$, same thing is

encountered in the three molecules. The CC bonds successively show the small values of ρ_c in this order with a clear difference between C5C6 and the rest of the bonds. The lack of symmetry due to the presence of a substituent at R17 in compounds 2 and 3 makes the six CC bonds different; this structural behavior essentially influences the electronic properties. The electronegative character of the nitrogen gives the C5C6 bond the lowest ρ_c values in the phenyl ring (Table 4).

3-4. Electrostatic potential

Table 5 groups together the electrostatic potential values for each atom of the molecules studied.

Table 5: Electrostatic Potential of Molecules

atom molecules	Q ₁	Q ₂	Q ₃
N ₁	-18.281921	-18.285143	-18.282925
C ₂	-14.624963	-14.628585	-14.625318
C ₃	-14.686816	-14.682465	-14.682296
N ₄	-18.335876	-18.347100	-18.344991
C ₅	-14.688794	-14.694106	-14.692354
C ₆	-14.666593	-14.672706	-14.671201
C ₇	-14.714847	-14.719105	-14.717775
C ₈	-14.714437	-14.719663	-14.718308
C ₉	-14.723946	-14.728364	-14.726997
C ₁₀	-14.722102	-14.727502	-14.726042
O ₁₁	-22.342442	-22.343952	-22.340611
H ₁₂	-0.989349	-0.992565	-0.990736
H ₁₃	-1.097496	-1.102416	-1.100972
H ₁₄	-1.098705	-1.102886	-1.101694
H ₁₅	-1.093047	-1.097449	-1.096286
H ₁₆	-1.082451	-1.086384	-1.085119
R ₁₇	-1.095530	-14.742069	-14.734464

As a side effect, it can be noted that the presence of the methyl and phenyl groups in the two compounds 2 and 3 respectively leads to a slight increase of V_c in the phenyl ring (compare the four values of the C5, C6, C8 and C9 atoms).

The changes induced in this cycle by the substitution of R17 show a slight increase of V_c in the nitrogen cycle except for the carbon atom C3 where a slight decrease is observed because of its proximity to the methyl and phenyl groups in the two compounds 2 and 3.

3-4. NPA Atomic Charge and Dipolar Moment

Figure 2, reveals the general model given by the NPA atomic charges of quinoxalin-2(1H)-one and its two derivatives (compounds 2 and 3). It can be seen from the analysis of this table that the C2 carbonyl carbon has the highest positive value of about +0.57e for the molecular 1. This value decreases by +0.01e and increases by +0.01e for the substitution with the methyl and benzyl groups, respectively. This is due to their proximity to both the nitrogen atom N1 and the oxygen atom O11. In fact, these last two atoms have high negative charges of the order of -0.64e and -0.51e respectively.

The increase in the charge density of C2 carbon for compounds 2 and 3 results in the appearance of high negative charges on the R17 group of about -0.35e for molecule 2 and -0.28e for molecule 3.

The C5 and C6 carbons shared by the two rings of the molecule are positively charged. This charge is due to their bonds to the two nitrogen atoms N1 and N4. As a result, the other phenyl carbons have negative charges which produce polarized CH bonds.

The effect of the substitution on these electronic populations can be summarized as follows: the methyl group in the compound 2 and the benzyl group in the compound 3 respectively substituted in the 3-position do not product the same qualitatively changes in the carbon atoms of the phenyl ring. According to the analysis of these results, the derivatives of quinoxalin-2(1H)-one represented by the NPA charges show that there is a polarization between the main carbonyl groups bonded to the nitrogen atoms and the phenyl ring.

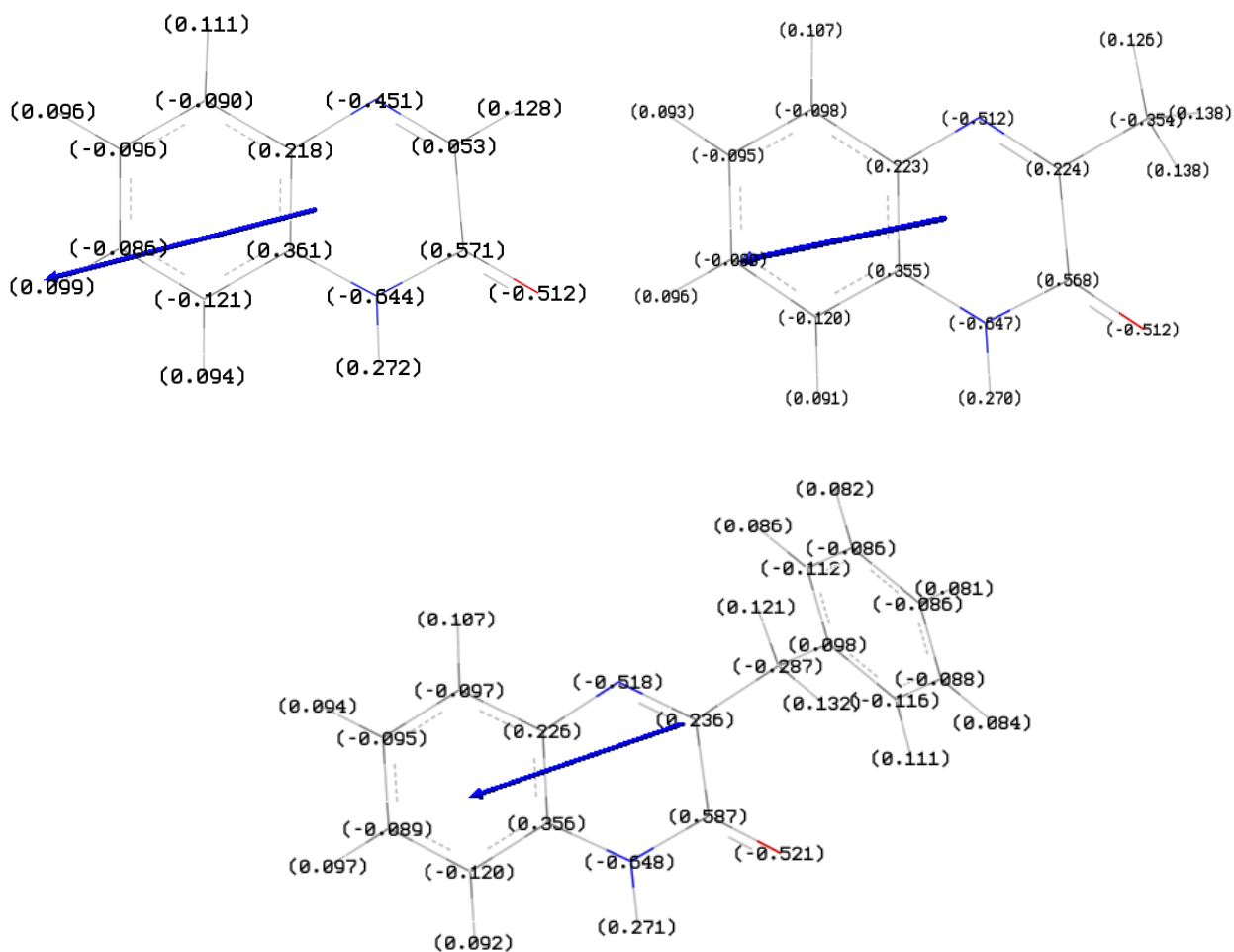


Figure.2: Dipolar moment vectors μ and the charge distribution for the three molecules Q1, Q2 and Q3 in the ground state calculated by the method DFT (B3LYP)/6-31G(d, p)

To confirm the polarization result obtained by analyzing the NPA charges values, we determined the dipole moment vectors μ in a three-dimensional representation of quinoxalin-2(1H)-one and its two isolated derivatives by the theoretical calculation method B3LYP/6-31G (d, p). Figure 4 shows the data thus obtained. The dipole moment vector μ has been compared to the standard orientation for each molecule, that is to say that the center of each nuclear charge is the origin of the coordinates.

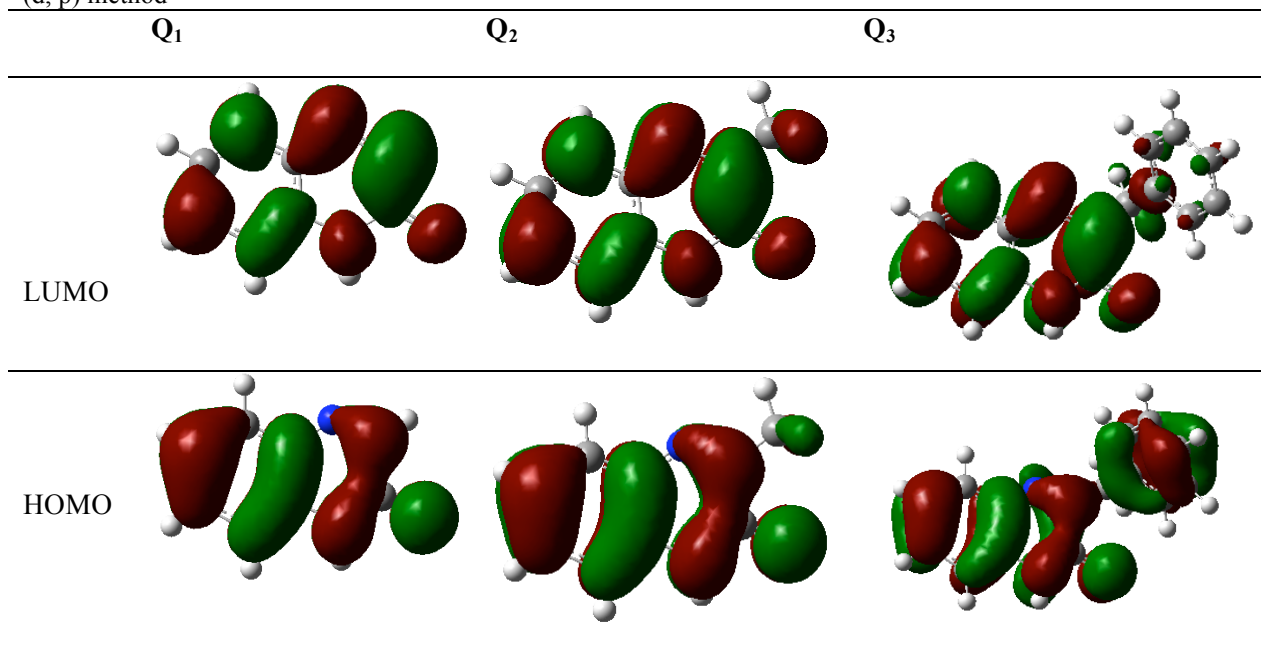
The dipolar momentum of the compound 1 (3.9607 Debye) decreases with the substitution of the R17 group by the methyl (compound 2) (3.0800 Debye) and the benzyl group (compound 3) (3.4194 Debye). However, the substitution makes not only to drastically reduce in the dipolar moment, but also to modify the orientation of the corresponding vector (Figure 4).

The information provided by the NPA charges as well as the change in dipole moment μ shows the effect of the substitution of the R17 group by methyl and benzyl in quinoxalin-2(1H)-one. This will allow to modify the reactivity of these molecules and resulting the modification of their effects of medical treatment in the pharmacological application field.

Table 6: Calculated values of the Q_1 and Q_2 and Q_3 global reactivity descriptors with the DFT (B3LYP)/6-31G (d, p) method in gas phase.

Descriptors	Q_1	Q_2	Q_3
E_T (eV)	-493.2150	-532.5425	-763.5982
μ (D)	3.9607	3.0800	3.4194
E_{HOMO} (eV)	-6.3275	-6.1941	-6.2050
E_{LUMO} (eV)	-1.9649	-1.7290	-1.8327
ΔE (eV)	4.3626	4.4651	4.3723

Table 7: Electronic densities of LUMO and HOMO orbital's of Q1 and Q2 and Q3 isolated with the DFT (B3LYP)/6-31G (d, p) method



The behavior of intramolecular charge transfer (ICT) has been obtained from the orbital molecular boundary (FMO) contribution [37, 38]. We have represented graphically the electronic spatial distribution of the HOMO and LUMO orbitals of all the dyes (Table 7). Generally, the HOMO and LUMO plots have demonstrated the typical molecular orbital characteristics of the π type. In addition, the HOMO displays an anti-stick character between two adjacent fragments and a link character within each unit. The LUMOs have the bonding character between the two adjacent fragments, so that the lowest singular states correspond to the electronic transition of the π - π^* type [39, 40]. As shown in Table 7, the model of HOMOs and LUMOs are qualitatively similar to each other, respectively. In addition, HOMO electron distributions are mainly located in the electron donor at the conjugated π spacing, whereas LUMOs are mainly located on the conjugation spacing fragment and the electron acceptor fragments. Therefore, the electron transitions of all D- π -A dyes from HOMO to LUMO could lead to ICT from the donor units to the acceptor groups / anchor by the conjugate bridge, so that the HOMO-LUMO transition can be classified as π - π^* ICT.

Conclusions

A first theoretical study carried out on quantum calculations with DFT/B3LYP/6-31G(d, p) level is presented for the molecule of quinoxalin-2(1H)-one and its two derivatives: 3-methylquinoxalin-2(1H)-one and 3-benzylquinoxalin-2(1H)-one. These molecules have a potential interest for the chemical reactivity of the relative compounds.

The analysis of various molecular properties according to electron density shows some essential properties to be considered in other studies on the chemistry of these molecules. The most suitable is the strong enhancement of the polarization of the carbonyl groups due to the presence of two neighboring nitrogen and a condensed phenyl ring. Substitution of R17 with methyl and phenyl is expected to significantly increase the reactivity of carbonyl in quinoxalin-2 (1H)-one and their derivatives.

The substitutions not only reduce the dipolar moment drastically, but also modify the orientation of the corresponding vector. The information provided by the NPA charges as well as the change in dipole moment μ , that shows the effect of the substitution of the R17 group by methyl and benzyl in quinoxalin-2(1H)-one.

Acknowledgments - Research Project Support Program(PPR 1127/16) – Morocco.

References

1. J. Ohmori, S. Sakamoto, H. Kubota, M. Shimizu-Sasamata, M. Okada, S. Kawasaki, K. Hidaka, J. Togami, T. Furuya, K. Murase, *J. med. Chem.* 37 (1994) 467-475.
2. J. R. Epperson, P. Hewawasam, N. A. Meanwell, C. G. Boissard, V. K. Gribkoff, D. Post-Munson, *Bioorg. Med. Chem. Lett.* 3 (1993) 2801-2804.

3. R. Nagata, N. Tanno, T. Kodo, N. Ae, H. Yamaguchi, T. Nishimura, F. Antoku, T. Tatsuno, T. Kato, *J. med. Chem.* 37 (1994) 3956-3968.
4. L. Turski, A. Huth, M. Sheardown, F. McDonald, R. Neuhaus, H. H. Schneider, U. Dirnagl, F. Wiegand, P. Jacobsen, E. Ottow, *Proc. Natl. Acad. Sci.* 95 (1998) 10960-10965.
5. G. W. Cheeseman, R. F. Cookson, *Chem. Heterocycl. Compd.*, 35 (1979).
6. Y. Kurasawa, A. Takada, *Heterocycles*, 23 (1985) 2083-2119.
7. S.-K. Lin, *Mol. Online*, 1 (1996) 37-40.
8. S.-K. Lin, *J. photochem.*, 37 (1987) 363-377.
9. H. Kawata, K. Kikuchi, H. Kokubun, *J. photochem.*, 21 (1983) 343-350.
10. A. Jarrar, Z. Fataftah, *Tetrahedron*, 33 (1977) 2127-2129.
11. G. Cheeseman, E. Törzs, *J. Chem. Soc. C: Org.* (1966) 157-160.
12. A. El Assyry, B. Benali, A. Boucetta, B. Lakhrissi, *J. Struct. Chem.* 55 (2014) 38-44.
13. H. Tayebi, H. Bourazmi, B. Himmi, A. El Assyry, Y. Ramli, A. Zarrouk, A. Geunbour, B. Hammouti, *Der. Pharm. Chem.* 6 (2014) 220-234.
14. B. Benali, Z. Lazar, A. Boucetta, A. El Assyry, B. Lakhrissi, M. Massoui, C. Jermoumi, P. Negrier, J. M. Léger, D. Mondieig, *Spect. Lett.* 41 (2008) 64-71.
15. A. El Assyry, B. Benali, B. Lakhrissi, M. El Faydy, M. E. Touhami, R. Tourir, M. Touil, *Res. Chem. Intermed.*, 41 (2015) 3419-3431.
16. R. Jdaa, B. Benali, A. El Assyry, B. Lakhrissi, *Opt. Quant. Electron.*, 49 (2017) 79.
17. N. Padmaja, S. Ramakumar, M. Viswamitra, *Acta. Crystallogr. Sect. C: Cryst. Struct. Commun.*, 43 (1987) 2239-2240.
18. D. Mondieig, P. Negrier, S. Massip, J. M. Leger, C. Jarmoumi, B. Lakhrissi, *J. Phys. Org. Chem.*, 24 (2011) 1193-1200.
19. L. Gracia et al. *Phys. Rev. B* 80, 094105 (2009); L. Gracia et al. *Inorg. Chem.* 51 (2012) 1751.
20. A. Benmakhlouf, *Dalton Trans.* 11 (2017) 5058.
21. C. Öğretir, B. Mihci, G. Bereket, *J. Mol. Struct. (Theochem)* 488 (1999) 223-231.
22. R. Soliva, M. Orozco, F. J. Luque, *J. Comput. Chem.* 18 (1997) 980-991.
23. R. Bader, A. I. Mol., *Clarendon: Oxf, UK* 1990.
24. P. Popelier, G. Logothetis, *Prentice Hall: Harlow, England*, (2000).
25. A. E. Reed, L. A. Curtiss, F. Weinhold, *Chem. Rev.* 88 (1988) 899-926.
26. P. Politzer, D. G. Truhlar, *Sci. Bus. Media.*, (2013).
27. K. B. Lipkowitz, D. B. Boyd, *Reviews in Compt. Chem.: Volume 13*, Wiley Online Library.
28. A. E. Reed, R. B. Weinstock, F. Weinhold, *J. Chem. Phys.* 83 (1985) 735-746.
29. K. B. Wiberg, P. R. Rablen, *J. Comput. Chem.* 14 (1993) 1504-1518.
30. L. Pacios, P. Gómez, *J. Mol. Struct. (Theochem)*, 544 (2001) 237-251.
31. M. Frisch, G. Trucks, H. B. Schlegel, G. Scuseria, M. Robb, J. Cheeseman, G. Scalmani, V. Barone, B. Mennucci, G. Petersson, *Inc. Wallingford CT* (2009) 200.
32. A. El Assyry, R. Jdaa, B. Benali, M. Addou, A. Zarrouk, *J. Mater. Environ. Sci.* 6 (2015) 2612-2623.
33. C. Lee, W. Yang, R. G. Parr, *Phys. Rev. B*, 37 (1988) 785-789.
34. A. D. Becke, *J. chem. Phys.* 98 (1993) 1372-1377.
35. M. Jellal, Y. Ramlia, A. Moussaïfa, Y. K. Rodib, J. Fifania, E. Essassia, M. Pierrotc, *J. Soc. Chim. Tunisie.*, 7 (2005) 19-26.
36. P. Popelier, F. Aicken, S. O'Brien, *Chem. Model.: Appl. Theory.*, 1 (2000) 143-198.
37. B. Benali, Z. Lazar, K. Elblidi, B. Lakhrissi, M. Massoui, A. Elassyry, C. Cazeau-Dubroca, *J. Mol. Liq.*, 128 (2006) 42-45.
38. A. El Assyry, B. Benali, A. Boucetta, Z. Lazar, B. Lakhrissi, M. Massoui, D. Mondieig, *Spect. Lett.*, 42 (2009) 203-209.
39. B. Benali, A. El Assyry, A. Boucetta, Z. Lazar, B. Lakhrissi, M. Massoui, D. Mondieig, *Spect. Lett.*, 40 (2007) 893-901.
40. A. Elassyry, B. Benali, Z. Lazar, K. Elblidi, B. Lakhrissi, M. Massoui, D. Mondieig, *J. Mol. Liq.*, 128 (2006) 46-49.

(2018) ; <http://www.jmaterenvironsci.com>